JOURNAL OF GEOPHYSICAL RESEARCH, VOL. 106, NO. B4, PAGES 6673–6682, APRIL 10, 2001

Deformation across the Pacific-North America plate boundary near San Francisco, California

William H. Prescott, James C. Savage, Jerry L. Svarc, and David Manaker[1]

U.S. Geological Survey, Menlo Park, California

Abstract. We have detected a narrow zone of compression between the Coast Ranges and the Great Valley, and we have estimated slip rates for the San Andreas, Rodgers Creek, and Green Valley faults just north of San Francisco. These results are based on an analysis of campaign and continuous Global Positioning System (GPS) data collected between 1992 and 2000 in central California. The zone of compression between the Coast Ranges and the Great Valley is 25 km wide. The observations clearly show 3.8±1.5 mm yr^{-1} of shortening over this narrow zone. The strike slip components are best fit by a model with 20.8±1.9 mm yr^{-1} slip on the San Andreas fault, 10.3±2.6 mm yr^{-1} on the Rodgers Creek fault, and 8.1±2.1 mm yr^{-1} on the Green Valley fault. The Pacific-Sierra Nevada-Great Valley motion totals 39.2±3.8 mm yr^{-1} across a zone that is 120 km wide (at the latitude of San Francisco). Standard deviations are one σ. The geodetic results suggest a higher than geologic rate for the Green Valley fault. The geodetic results also suggest an inconsistency between geologic estimates of the San Andreas rate and seismologic estimates of the depth of locking on the San Andreas fault. The only convergence observed is in the narrow zone along the border between the Great Valley and the Coast Ranges.

1. Introduction

Central California is located on the boundary between the North America plate and the Pacific Plate. The relative motion of the North America and Pacific plates is accommodated over a broad region. The San Andreas Fault System in the Coast Ranges forms the western side of this region. The Great Basin forms the eastern side [*Bennett et al.*, 1998; *Thatcher et al.*, 1999]. Between them lies a relatively rigid microplate, the Sierra Nevada-Great Valley [*Argus and Gordon*, 1991a]. It has long been recognized that motion on the San Andreas system did not account for all of Pacific-North America motion [*Atwater*, 1970]. In this paper we use the velocities of geodetic stations to estimate both slip rates on San Andreas system faults and convergence between the Great Valley and the Coast Ranges.

2. Data

Our data came from four sources: the Bay Area Regional Deformation Network (BARD), Continuously Operating Reference Stations (CORS), U.S. Geological Survey (USGS) campaign observations, and International GPS Service (IGS). BARD is a regional network of stations involving a consortium of institutions in Central California (University of California, Berkeley, U.S. Geological Survey, University of California, Davis, Stanford University, and Trimble Navigation). BARD spans the Sierra Nevada-Great Valley microplate, the San Andreas Fault System, and the edge of the Pacific plate (Figures 1 and 2). There are a few CORS [*Snay and Weston*, 1999] stations in the area and these have been included in our analysis. The U.S. Geological Survey has made campaign-style GPS measurements on a profile of stations transecting the San Andreas Fault System in the vicinity of San Francisco Bay (Figures 1 and 2). IGS stations (see also http:// lareg.ensg.ign.fr/ITRF/itrf96.html) were used to control the reference frame. Their velocities are not listed. Details about the processing are given below.

We examined the motion of 30 stations transecting the San Andreas Fault System and the Sierra Nevada Great Valley microplate. Stations in the San Andreas Fault System form a profile normal to the trends of the faults. These Coast Range stations should be relatively unaffected by along-strike variations in the faults. Stations on the Sierra Nevada Great Valley microplate are widely distributed.

Table 1 summarizes the observation history of all the stations. Observed phase data from the stations was divided into daily bins. GPS Inferred Positioning System (GIPSY) software [*Zumberge et al.*, 1997] was used to obtain a daily position for each station. These daily solutions were run in a "point positioning mode" using clock corrections and orbits from the NASA/Caltech Jet Propulsion Laboratory. The point positions for the local stations were merged into a single combined solution; then, the phase ambiguities for these local stations were resolved in a network-processing mode.

There are 51 "core" IGS stations. Typically, data were available from ~30 of these on any given day. For each day that we had a local position, we calculated point positions for all the available core IGS stations. These stations were used to control the reference frame of our solutions (see next paragraph). No attempt was made to resolve ambiguities for these IGS stations. The processing produced loosely

[1]Now at Dept. of Geology, University of California, Davis, California.

Paper number 2000JB900397.

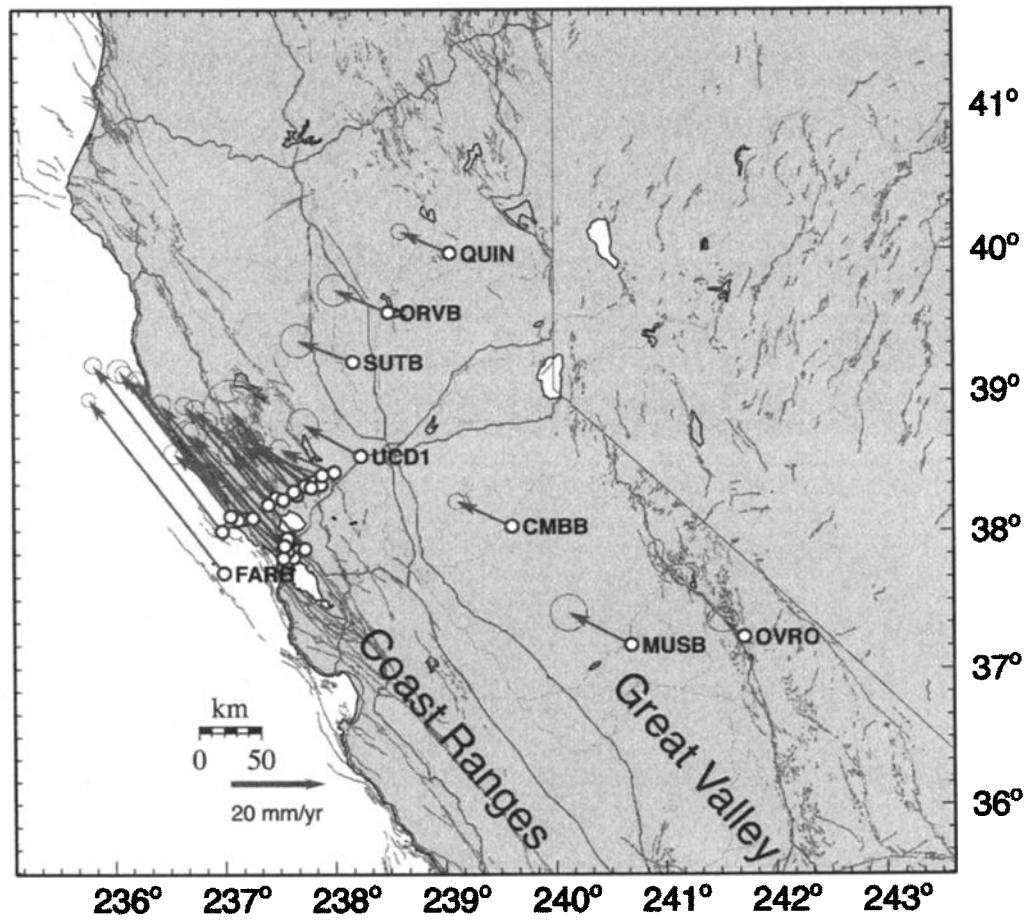

Figure 1. Small-scale map of stations and their velocities. Error ellipses are 95% confidence.

constrained positions for all of the central California stations and for this subset of the IGS stations. Because these solutions were not tied to any reference frame, the position of a station varied from day to day.

In order to obtain velocities relative to "stable North America" we removed this reference frame uncertainty as follows: The starting point was the International Terrestrial Reference Frame (ITRF97) [*Boucher et al.*, 1996] (see also ITRF96 results). ITRF97 specifies positions and velocities for several hundred IGS stations, including the 51 that we routinely processed. The ITRF97 reference frame velocities were derived by minimizing the differences with ITRF96 velocities, and these in turn were derived by minimizing the differences with NUVEL1-NNR velocities [*Argus and Gordon*, 1991b]. Thus ITFR97 velocities are essentially in the NUVEL1-NNR reference frame. (See http:// lareg.ensg.ign.fr/ ITRF/ ITRF97/ itrf97-in/ itrf97-in.html#analysis for more details.)

We then picked 12 North American stations (ALGO, BRMU, CHUR, DRAO, GODE, KELY, MDO1, NLIB, RCM5, STJO, THU1, WES2, and YELL) to define the motion of "stable North America." These 12 are all located on the North America plate and removed from plate boundaries. We found that FAIR and PIE1, both nominally on stable North America, appeared to have significant velocities relative to the other stations, so neither of these was included. On the other hand, DRAO appeared consistent with the other 11, so it was included, even though it is located near the North America-Juan de Fuca plate boundary. The ITRF97 velocities, (see also ITRF96 results), for these 12 stations were used to compute a best fitting Euler pole for NA-ITRF97. The best fitting pole is located at 2.2±0.9° S, -80.0 ±0.4° E, with a rotation rate of 0.197±0.003°/Myr. For comparison [*DeMets and Dixon*, 1999], found a very similar location for the NA-ITRF96 pole (0.9±4.1° S, -79.8±1.6 ° E, 0.192±0.009°/Myr). The predicted motion about this Euler pole was subtracted from all 51 of the IGS stations, producing a "stable" North America reference frame. Finally, each daily solution for the California and IGS stations was rotated and translated (seven parameter Helmert transformed) into the configuration most closely approximating the reference frame. The result of this process was a series of positions for each station relative to stable North America.

Typical time series are shown in Figures 3 and 4. The BARD stations operate continuously. However, in order to reduce the processing time required, we generally only processed one solution per week. Weekly solutions provide more than enough data to provide estimates of the velocities. In the case of profile stations observed in campaign mode, all of the data were processed. Typically, these stations are observed on 2 consecutive days, once a year. Repeatability can best be judged from the continuous stations. We estimated repeatability from the RMS residual about the best fit to the time series for a single station assuming that changes in the

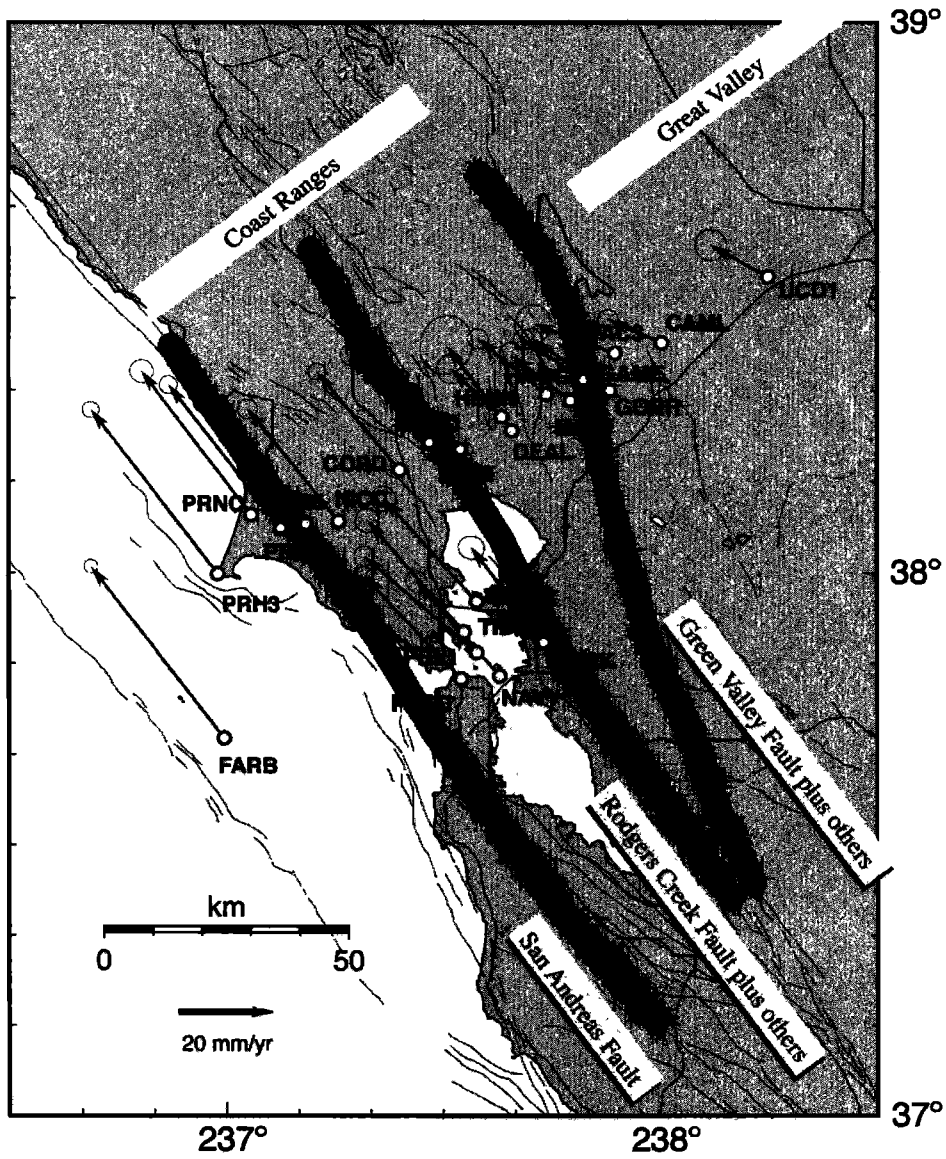

Figure 2. Large-scale map of stations near the Coast Ranges and their velocities. Error ellipses are 95% confidence. Highlight indicates faults included in the model.

position are linear with time. We found that station components had a typical repeatability of ~3, 5, and 15 mm in the north, east, and up components, respectively.

All of the errors used in this discussion are derived as follows: we started with the formal errors obtained in the GIPSY solutions. These were scaled by a factor of 2.0 to produce a scaled formal error level that approximates the observed RMS about the linear fit to the time series. Errors in the velocities were then calculated by assuming that there were two sources of error. The first source is Gaussian and was estimated from the scaled formal errors (propagating them through the velocity calculation). The second source is a random walk motion of the station. The magnitude of random walk error is probably station-dependent and is very poorly known. We have assumed that the random walk component was 1.0 mm $yr^{-1/2}$. This estimate is consistent with typical values [*Johnson and Agnew*, 1995]. However, it is a very poorly constrained number. Velocities were calculated using the quasi observation combinatorial analysis (QOCA) processing package [*Dong et al.*, 1998]. (Plots of the observed data for all of the stations can be found on the web at http://quake.usgs.gov/docs/deformation/NorthSanFranciscoBay.)

3. Discussion

Fault-parallel shear and fault-normal convergence are most easily seen in a coordinate system aligned along the predominant fault direction. In Figure 5 and Table 2, we resolve the motion of the stations into components parallel and normal to the direction of NUVEL1A-NNR plate motion [*DeMets et al.*, 1994] at San Francisco (N33.85°W). The profile crosses three major right-lateral strike slip faults, the San Andreas, Rodgers Creek, and Green Valley faults [*Jennings*, 1994]. The dominant signal in Figure 5 is the shear strain accumulating in the fault-parallel component over the Coast Ranges, near the San Andreas System faults (abscissa -

Table 1. Stations, Locations, Observation Histories, and Velocities[a]

Station	Latitude, °N	Longitude, °E	History			ITRF97		NoAm		1-σ	
			N	First	Last	V_n	V_e	V_n	V_e	S_n	S_e
1395	38° 05' 14.309"	-122° 48' 45.515"	9	1993	1998	14.2	-33.3	29.1	-22.8	0.8	0.8
ADOO	38° 14' 11.117"	-122° 31' 38.880"	8	1993	1998	3.9	-27.5	18.7	-16.9	0.8	0.8
AIRR	38° 13' 23.463"	-122° 27' 20.416"	9	1993	1998	1.7	-26.4	16.5	-15.8	0.8	0.8
CAML	38° 25' 00.047"	-121° 59' 40.950"	8	1993	1998	-9.6	-22.1	5.0	-11.4	0.9	0.9
CMBB	38° 02' 03.035"	-120° 23' 09.736"	340	1994	2000	-8.9	-22.6	5.2	-11.7	0.7	0.7
CORD	38° 11' 09.568"	-122° 35' 43.022"	15	1993	1998	6.2	-28.3	21.0	-17.7	0.7	0.8
DEAL	38° 15' 28.123"	-122° 20' 16.712"	5	1996	1998	3.6	-24.6	18.3	-14.0	2.5	2.3
FARB	37° 41' 49.941"	-123° 00' 02.747"	378	1994	2000	21.7	-38.7	36.6	-28.3	0.6	0.6
GAME	38° 21' 02.466"	-122° 10' 30.879"	8	1994	1998	-6.1	-23.3	8.6	-12.6	0.8	0.9
GORR	38° 19' 52.242"	-122° 06' 52.579"	11	1993	1998	-3.7	-27.3	11.0	-16.6	0.9	0.9
HAGG	38° 19' 25.960"	-122° 15' 33.123"	8	1993	1998	-2.9	-25.1	11.8	-14.5	0.8	0.8
HENN	38° 16' 59.542"	-122° 21' 42.303"	5	1993	1996	-4.6	-21.4	10.1	-10.8	1.2	1.2
MADI	38° 18' 45.383"	-122° 12' 11.486"	7	1994	1998	-5.0	-23.3	9.7	-12.6	1.1	1.1
MOLA	37° 56' 47.667"	-122° 25' 11.717"	228	1994	2000	7.1	-30.3	21.9	-19.8	1.1	1.1
MUSB	37° 10' 11.788"	-119° 18' 33.653"	128	1997	2000	-7.0	-24.0	6.9	-13.2	1.6	1.6
NAVY	37° 48' 35.855"	-122° 21' 58.158"	10	1993	1998	5.5	-28.2	20.2	-17.7	0.9	0.9
NICC	38° 05' 33.552"	-122° 44' 11.547"	8	1993	1998	9.2	-29.8	24.0	-19.3	0.8	0.8
ORVB	39° 33' 16.660"	-121° 30' 01.039"	185	1996	2000	-9.6	-22.4	4.9	-11.4	1.4	1.4
OVRO	37° 13' 55.167"	-118° 17' 00.863"	10	1994	1998	-10.0	-15.5	3.6	-4.5	1.1	1.4
PBL1	37° 51' 10.993"	-122° 25' 08.199"	236	1995	2000	5.8	-34.5	20.6	-24.0	0.9	0.9
PRH2	38° 04' 46.957"	-122° 52' 07.415"	13	1993	1998	15.8	-34.5	30.7	-24.0	0.8	0.8
PRH3	37° 59' 47.059"	-123° 00' 53.653"	20	1993	1998	20.2	-37.5	35.1	-27.0	0.7	0.7
PRNC	38° 06' 12.694"	-122° 56' 11.747"	12	1993	1996	15.9	-33.9	30.8	-23.4	1.0	1.0
PRSD	37° 48' 19.092"	-122° 27' 18.254"	21	1993	1998	7.1	-31.2	21.9	-20.7	0.8	0.8
QUIN	39° 58' 28.396"	-120° 56' 39.933"	304	1994	2000	-9.7	-21.6	4.6	-10.4	0.7	0.7
SUTB	39° 12' 21.012"	-121° 49' 14.148"	161	1997	2000	-10.1	-22.6	4.5	-11.7	1.4	1.4
TIBB	37° 53' 27.146"	-122° 26' 51.356"	297	1994	2000	9.1	-31.1	23.9	-20.6	1.1	1.1
UCBK	37° 52' 18.435"	-122° 15' 54.543"	7	1993	1998	5.6	-25.9	20.3	-15.4	1.0	1.1
UCD1	38° 32' 10.464"	-121° 45' 04.424"	138	1996	2000	-7.9	-23.0	6.7	-12.2	1.3	1.3
VAC3	38° 23' 52.358"	-122° 06' 10.514"	11	1995	1998	-8.4	-28.0	6.2	-17.3	1.7	1.6

[a]The number of observations N counts each day separately. For example, DEAL was observed once in 1996, then on two days in fall 1997 and two days in December 1998, for a total of five observations. V_n is north component of velocity relative to ITRF97 or North America (NoAm). V_e is east component of velocity relative to ITRF97 or NoAm. S_n and S_e are the one-standard deviation uncertainties. The 1-σ error columns apply to both the ITRF97 and NoAm velocities since we assume this transformation is exact.

50 to ~100 km). In the Great Valley (100 to 200 km), there is no shear. In both sections the motion normal to the plate motion direction is much smaller. Slip rates for the three faults were obtained from two-dimensional modeling.

3.1. San Andreas System Shear Deformation

The GPS stations form a profile that crosses the San Andreas shear zone at the northern end of San Francisco Bay. At this latitude the principal faults comprising the shear zone are the Green Valley, Napa, Rodgers Creek, and San Andreas. Paleoseismic observations [*Working Group on California Earthquake Probabilities*, 1999] (hereinafter referred to as WG99) for the San Andreas, Rodgers Creek, and Green Valley faults indicate that all three have significant rates of motion over the past few thousand years. Other studies have examined the contemporary distribution of motion in this area [*Lisowski et al.*, 1991; *Prescott and Yu*, 1986]. We now have a longer observation history for many stations and data from stations that were not available previously.

Our modeling effort incorporated the following assumptions: (1) the fault model is two dimensional [*Chinnery*, 1961]; (2) the earth is treated as a linear elastic half space; (3) the faults are locked at the surface and assumed to be slipping below some depth, that is, the faults are modeled with infinite screw dislocations buried at the locking depth; (4) the modeled faults are San Andreas, Rodgers Creek and Green Valley; and (5) in addition to the fault deformation, the station velocities contain rigid-body components. This rigid-body motion primarily results from motion of Sierra Nevada-Great Valley microplate relative to North America but may contain other sources of reference frame uncertainty.

We considered four classes of models: (1) solve for both slip rates and locking depths; (2) specify slip rates and solve for locking depths; (3) specify locking depths and solve for slip rates (preferred model); (4) specify locking depths, solve for slip rates and creep rates.

Mathematica and its implementation of the Levenberg-Marquardt method was used for inversions, both linear and nonlinear [*Wolfram*, 1996]. (Surface deformation is a linear function of slip rate but a nonlinear function of the locking depth). Our preferred model (Table 3) was obtained with the locking depths constrained to WG99 values, the slip rates on three faults estimated, and no creep allowed. Before discussing the preferred model, we will describe the results that led us to reject alternate models.

Attempts to estimate the locking depths and the slip rates simultaneously (model 1) produced poorly constrained results. The strong correlation between slip rate and locking depth makes them difficult for the inversion to separate. With slip rates constrained to WG99 values (model 2) the uncertainties in some of the locking depths were large (Table 3). This solution did not fit the data as well as our preferred model (overall estimated normalized variance was 15% larger), and we rejected it for these reasons.

We considered a model that included creep near the surface on the Green Valley fault (model 4). The solution found a

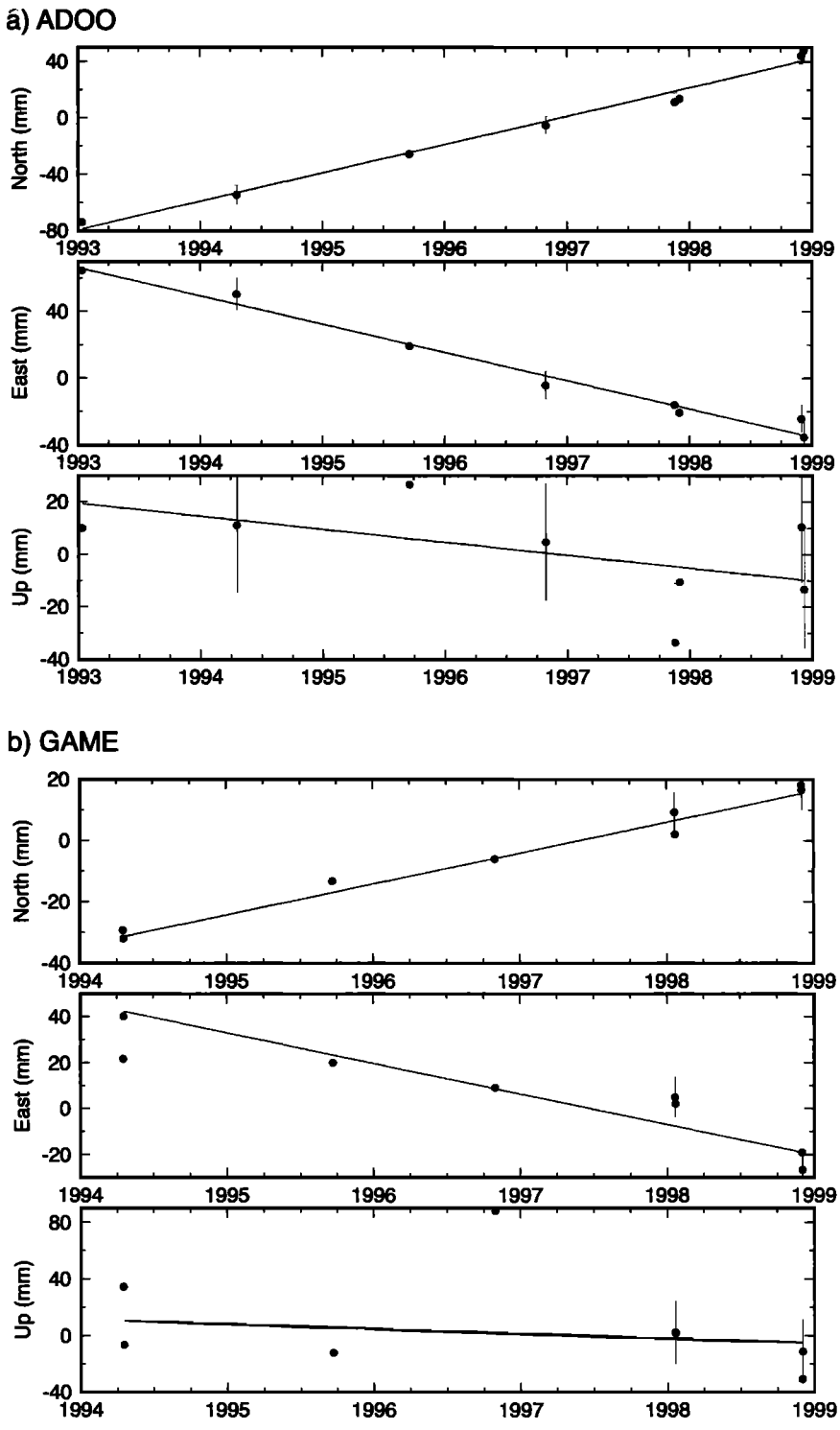

Figure 3. Time series for two stations observed in campaign mode. Error bars indicate plus and minus one standard deviation. The vertical scale is different for different components. The time period spanned by the data is different for the two stations. The up component was not used in this analysis but is included for completeness.

negative value for the creep rate on the Green Valley fault. The fault runs between station MADI (velocity 15.1 mm yr^{-1}) and GAME (velocity 14.2 mm yr^{-1}). However station GORR, located just a few kilometers further northeast of the Green Valley fault has a velocity of 18.4 mm yr^{-1}. Station GORR dominated the creep calculation and forced a left-lateral solution. We conclude that there is no evidence in the geodetic data for creep on the Green Valley fault. The uncertainty in the Green Valley fault creep rate depends on the assumed depth of creep. If the creep depth is taken as 5 km, the uncertainty in the model estimate of creep is 2.7 mm yr^{-1} at the 1 σ level. If the creep depth is only 1 km, the

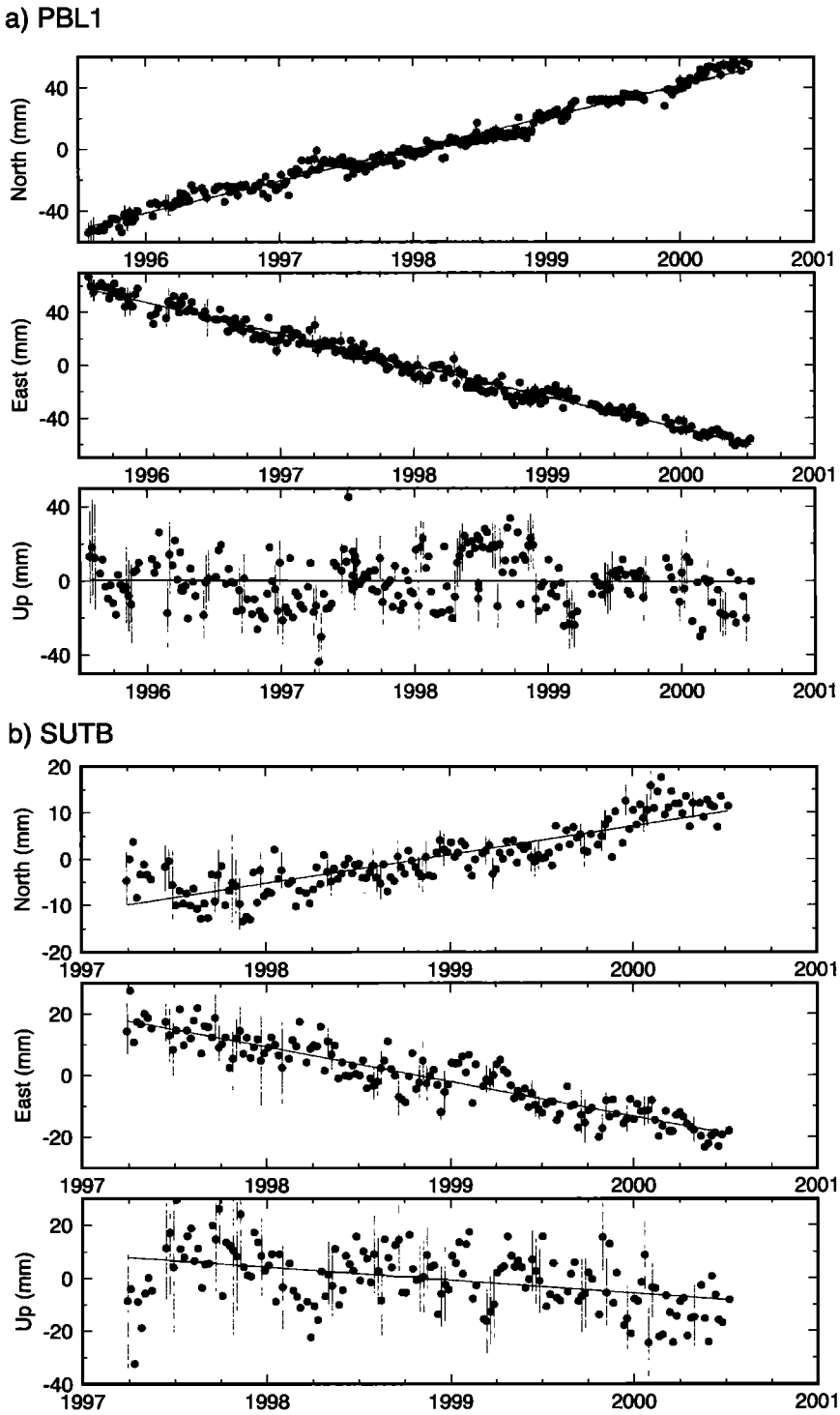

Figure 4. Time series for two continuous stations. PBL1 is a CORS station. SUTB is a BARD station. Error bars indicate plus and minus one standard deviation. The vertical scale is different for different components. The time period spanned by the data is different for the two stations. The up component was not used in this analysis but is included for completeness.

uncertainty goes up to 4.7 mm yr^{-1}. So we cannot rule out the possibility of creep on the Green Valley fault, but the geodetic data certainly do not require it.

The data are consistent with the locking depths suggested by seismicity [*Working Group on California Earthquake Probabilities*, 1999], and in our preferred model (model 3) the depths were constrained to the depths adopted by the WG99. Given the assumed locking depths, slip rates on the three faults were well resolved by the best fitting model (Table 3 and Figure 5). This model predicts almost all the observations within two standard deviations. The exceptions are HENN and OVRO (abscissae are 44.7 and 279.1 km). OVRO is located east of the Owens Valley fault zone [*Dixon et al.*, 1995], and its motion relative to other stations in our analysis

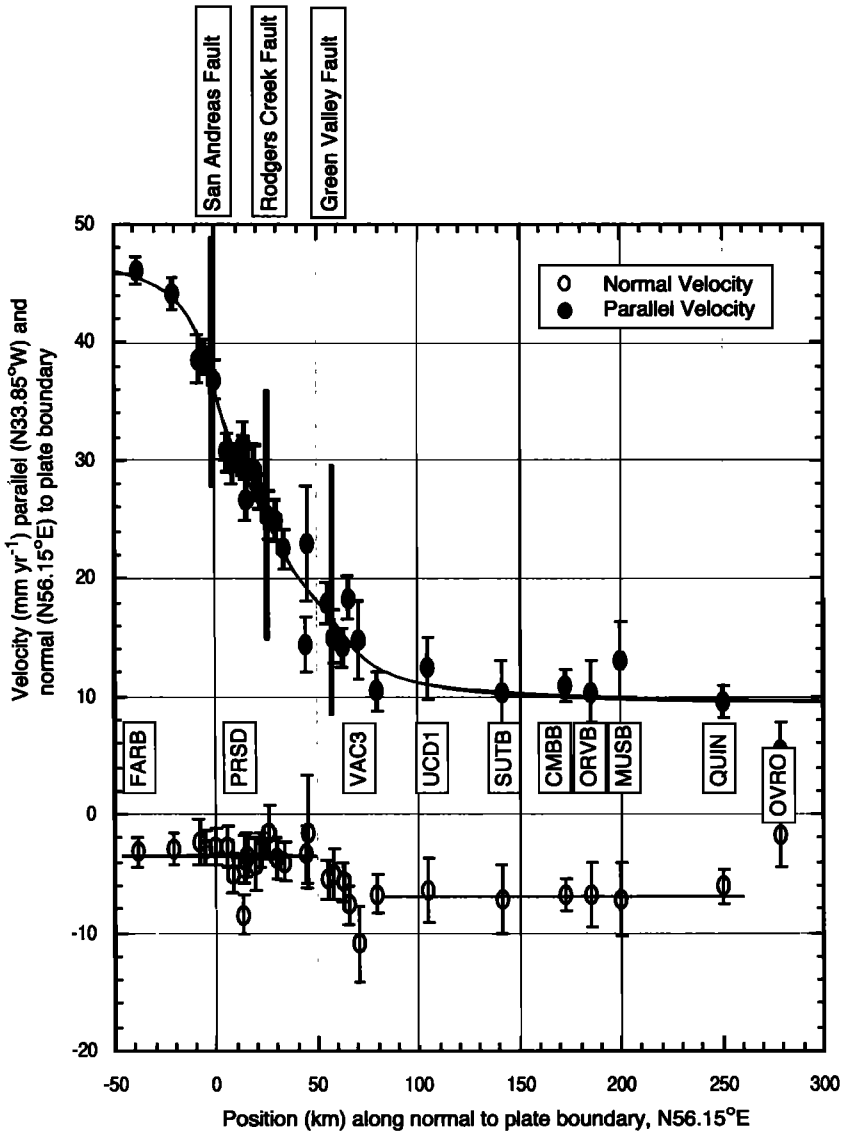

Figure 5. Plot of the motion of stations resolved into components parallel and normal to the observed direction of Pacific-North America motion (N33.85°W). Solid dots indicate the motion parallel to the direction of plate motion. Open dots indicate the motion normal to the direction of plate motion. The Pacific plate is at the left; the Sierra Nevada plate is at the right. The smooth curve through the fault-parallel component is the deformation predicted by the best fitting model (Table 3). Error bars indicate 2 σ errors.

is not properly modeled. We have no explanation for the anomalous motion of HENN. Owing to the impending destruction of HENN, it was replaced by station DEAL in 1996. Both were observed on November 13, 1996. HENN was observed four times between 1993 and 1996. DEAL was observed three times between 1996 and 1999. The overall estimated normalized variance of the best fitting model was 0.96, indicating that essentially all the model misfit can be attributed to the uncertainty in the observations. The inferred slip rates are slightly different than the paleoseismologic estimates used in WG99. In particular, the slip rate inferred for the San Andreas fault (20.8±1.9 mm yr^{-1}) is somewhat lower than the WG99 rate fault (24 mm yr^{-1}). And, the Green Valley fault rate (8.1±2.1 mm yr^{-1}) is somewhat higher than the WG99 rate fault (5 mm yr^{-1}).

Table 4 compares the rates obtained by several geodetic studies and the consensus rate given by WG99. Freymueller [1999] looked at stations located ~100 km to the north of those considered here. Williams [1995] examined a superset of the stations considered here. The data that Williams examined spanned the time period from ~1989 to 1993. Since that time, there have been significant improvements in GPS receivers (code-correlating 12-channel receivers have replaced the codeless or 4-channel receivers in use earlier). Also with the advent of IGS the orbits and reference frames are much better now than they were then. The total paleoseismologic slip rate equals the total given by the recent determinations of geodetic rate. However, in distributing the slip between the various faults the paleoseismologic rates differ from all of the geodetic studies (Table 4). The geodetic estimates put less of the slip on the San Andreas fault and more on the Green Valley fault (or its extension, the Bartlett Springs fault, see Freymueller et al.).

The difference in rates for the Green Valley/Bartlett

Table 2. Observed Station Velocities Resolved Into Components Parallel and Normal to the NUVEL1A-NNR Direction of Relative Motion Between Pacific and North America at San Francisco[a]

Station	Normal Position, km	Parallel Position, km	Normal Velocity, mm yr^{-1}	Parallel Velocity, mm yr^{-1}	Normal σ, mm yr^{-1}	Parallel σ, mm yr^{-1}
FARB	-38.6	36.4	-3.2	46.2	1.2	1.2
PRH3	-20.8	64.5	-2.9	44.2	1.4	1.4
PRNC	-8.3	70.6	-2.3	38.6	2.0	2.0
PRH2	-4.9	65.1	-2.8	38.9	1.5	1.5
1395	-0.3	63.0	-2.7	36.9	1.6	1.6
NICC	5.6	59.8	-2.7	30.7	1.7	1.7
PRSD	8.1	19.6	-4.9	29.7	1.6	1.6
PBL1	13.7	22.2	-8.4	30.5	1.7	1.7
TIBB	14.0	27.1	-3.8	31.3	2.1	2.1
NAVY	14.8	15.7	-3.4	26.7	1.8	1.8
MOLA	19.5	30.9	-4.2	29.2	2.2	2.2
CORD	21.7	61.5	-3.0	27.3	1.5	1.5
UCBK	26.1	16.4	-1.5	25.4	2.2	2.1
ADOO	29.8	62.8	-3.7	24.9	1.7	1.7
AIRR	34.1	58.1	-4.0	22.5	1.6	1.6
HENN	44.7	59.1	-3.3	14.4	2.4	2.4
DEAL	44.9	55.6	-1.4	23.0	4.7	4.9
HAGG	54.7	57.8	-5.5	17.9	1.7	1.7
MADI	58.1	54.1	-5.1	15.1	2.1	2.2
GAME	62.5	56.2	-5.7	14.2	1.7	1.7
GORR	65.6	51.5	-7.6	18.4	1.7	1.8
VAC3	70.6	57.1	-10.9	14.8	3.2	3.3
CAML	79.6	53.5	-6.7	10.5	1.7	1.7
UCD1	104.7	52.8	-6.4	12.4	2.7	2.7
SUTB	141.1	118.1	-7.2	10.3	2.9	2.9
CMBB	173.0	60.4	6.8	10.9	1.4	1.4
ORVB	185.5	135.0	-6.8	10.4	2.7	2.7
MUSB	200.0	-194.3	-7.2	13.1	3.2	3.2
QUIN	250.7	147.5	-6.1	9.6	1.4	1.4
OVRO	279.1	-239.0	-1.8	5.5	2.6	2.3

[a] Parallel direction is N33.85ßW. Normal direction is N56.15ßE.

Springs fault are not too surprising. The WG99 rate for the Green Valley fault is based a paleoseismologic rate of 3.4±0.3 mm yr^{-1} for the Concord fault to the south and an 18 year alignment array record on the Green Valley fault indicating creep at 4.9 mm yr^{-1} [*Working Group on California Earthquake Probabilities*, 1999]. It seems quite possible that there are multiple active strands for these faults. In that case the geodetic results will give an integrated sum of slip on multiple faults and the rates would not be directly comparable to paleoseismologic rates.

Table 3. Slip Rates and Locking Depths From WG99 and From the Geodetic Modeling[a]

	Slip rate, mm yr^{-1}	σ, mm yr^{-1}	Locking Depth, km	Depth σ, km
WG99 values				
San Andreas	24.0	1.5	11.0	1.0
Rodgers Creek	9.0	1.0	12.0	1.0
Green Valley	5.0	1.5	14.0	1.0
SNGV	n/a	n/a	n/a	n/a
Pac-NA	n/a	n/a	n/a	n/a
Model 2 (fix rates, estimate depths)				
San Andreas	24.0	-	13.8	2.2
Rodgers Creek	9.0	-	5.9	3.1
Green Valley	5.0	-	6.4	7.9
SNGV	10.4	0.4	n/a	n/a
Pac-NA	48.4	0.4	n/a	n/a
Model 3 (preferred, fix depths, estimate rates)				
San Andreas	20.8	1.9	11.0	-
Rodgers Creek	10.3	2.6	12.0	-
Green Valley	8.2	2.1	14.0	-
SNGV	9.0	0.7	n/a	n/a
Pac-NA	48.3	1.2	n/a	n/a
Mixed model (see text)				
San Andreas	24.0	-	14.5	2.4
Rodgers Creek	9.0	2.2	12.0	-
Green Valley	7.8	2.2	14.0	-
SNGV	8.8	0.7	n/a	n/a
Pac-NA	49.6	1.4	n/a	n/a

[a] A value in the σ column indicates that the corresponding parameter was estimated from the inversion. A "-" in a σ column indicates that the corresponding parameter was fixed in the inversion. "n/a" indicates that the entry in not applicable. σ is one standard deviation.

The paleoseismologic and geodetic rates for the San Andreas fault are somewhat different as well (Table 4). We suspect that the geodetic data may be underestimating the San Andreas slip rate; there are only a few stations located west of the San Andreas fault. If our model underestimates San Andreas slip, it will also underestimate the total slip. As noted above, the slip rates are strongly correlated with locking depth. We computed a mixed solution in which the San Andreas slip rate was fixed at the paleo-seismologic rate and the fault depth was allowed to vary. This model gave us a value of 14.5±1.4 km for the San Andreas locking depth. It fit the observations as well as our preferred model. Essentially, the geodetic data are suggesting that the paleoseismolgic rate for the San Andreas and the seismologic locking depth for the San Andreas are inconsistent. Either one can fit the geodetic data but not both.

Table 5 compares the Pacific-North America plate motion derived from our model with the Pacific-North America plate

Table 4. Comparison of Slip Rates from Various Analyses[a]

	This paper	Freymueller [1999]	Williams [1995] 2-D	Williams [1995] 3-D	WG99 [1999]
SA	20.8±1.9	17.4±2.8	16.7±1.4	18.1±1.2	24.0±1.5
RC	10.3±2.7	13.9±3.4	12.3±1.2	10.8±1.0	9.0±1.0
GV	8.1±2.2	8.2±2.0	7.0±0.7	7.5±1.2	5.0±1.5
Total	39.2±1.2	39.6±1.1	36.0	36.4±2.0	39.0

[a] Uncertainties are one σ.

Table 5. Pacific-North America Plate Motion Rate[a]

Study	Rate, mm yr^{-1}	Direction, °NW
Observed (this paper)	48.3	37.6
NUVEL1A [*Argus and Gordon*, 1991b]	46.6	33.8
Demets and Dixon [1999]	50.3	36.8

[a] The rate quoted for this study was obtained by summing the individual fault rates (Tab. 4) and adding the rigid offset relative to North America (9.0±0.7 mm-yr^{-1}). Rates quoted for the DeMets and Dixon and for the Argus and Gordon studies were obtained by calculating the motion of station FARB about the respective Pacific-North America Euler pole. One σ standard deviation for all values is at the 1 mm yr^{-1} and 1° level.

motion implied at this location by two other studies [*Argus and Gordon*, 1991b; *DeMets and Dixon*, 1999]. Our relative plate rate is ~2 mm yr^{-1} less than the current best estimate [*DeMets and Dixon*, 1999]. However, the mixed model in Table 4, brings the plate rate closer to the DeMets and Dixon estimate. If this interpretation is correct, then the total slip across the San Andreas System faults should probably be 40.8±3.4 mm yr^{-1} instead of the 39.2±3.8 mm yr^{-1} in Table 4.

3.2. Fault Normal Compression

There is clearly a much smaller signal in the fault-normal component of motion (Figure 5). There is no indication of a slope in the component, as would be expected if there were uniform contraction (negative slope in Figure 5) or extension (positive slope) occurring across the network. However, a clear transition occurs along the boundary between the Coast Ranges and the Great Valley (abcissa is 45 to 70 km). In the Coast Ranges the mean normal component is -3.4±1.5 mm yr^{-1}. Across the Great Valley, the rate is -7.2±1.5 mm yr^{-1}. We omitted OVRO from this calculation since it is separated from the Great Valley by the Owens Valley fault. Over the 25 km between the Coast Ranges and the Great Valley the contraction rate is 0.15±0.1 μ strain yr^{-1}, accommodating 3.8±1.5 mm yr^{-1} of shortening. This zone of shortening is also readily apparent in the vectors (Figures 1 and 2). This 25 km zone spans the edge of the Great Valley, a locale that is characterized by a series of thrust faults [*Jennings*, 1994]. There were two earthquakes in this zone near Winters, California, in 1892 [*Bakun*, 1999], and the Coalinga and Kettlement Hills earthquakes occurred in this boundary [*Bennett and Sherburne*, 1983]. Plate motion solutions, geomorphology, and stress solutions all have suggested that the Coast Ranges should be experiencing compression, but previous geodetic work across the Coast Ranges [*Lisowski et al.*, 1991] has failed to provide clear evidence of this contraction and, in fact, has appeared to rule it out. If our inferences from Figure 5 are correct, the explanation may be simple: All of the shortening is being accommodated along the edge of the Coast Ranges, with no compression in the Coast Ranges proper. Such a model would not preclude fault geometry-induced compression as hypothesized by recent studies [*Argus and Gordon*, 1996].

4. Conclusions

The slip rates for the San Andreas, Rodgers Creek, and Green Valley faults are 20.8±1.9, 10.3±2.6, and 8.1±2.1 mm yr^{-1}, respectively. The geodetic data do not support the observation that there is significant creep occurring along the Green Valley fault. The geodetic rate for the San Andreas fault is slightly lower than the paleoseismologic rate (24.0 mm yr^{-1}). The geodetic model also underestimates the total Pacific-North America plate motion rate by ~2 mm yr^{-1}. An alternate model, using the paleoseismologic rate as a constraint, agrees better with the plate rate. If this interpretation is correct, then the total slip across the San Andreas System faults should probably be 40.8±3.4 mm yr^{-1} instead of the 39.2±3.8 mm yr^{-1} implied by the above rates.

We have detected about 4 mm yr^{-1} of shortening along the edge of the Great Valley. At the latitude of San Francisco, this shortening is accommodated over a very narrow zone some 25 km in width normal to the trend of the faults.

Acknowledgments. We acknowledge the contributions of G. Hamilton, N. King, C. Stiffler, J. Sutton, J. Svarc, and K. Wendt and past members of the Crustal Strain Project at the USGS. We also acknowledge B. Romanowicz, R. Burgmann, M. Murray, and R. Baxter for their contributions to the BARD project and data set. We thank the many individuals responsible for IGS and CORS for making their data available to us. The paper benefited from the reviews of J. Freymueller, J. Lienkaemper, S. Owen, R. Simpson, and an anonymous reviewer.

References

Argus, D.F., and R.G. Gordon, Current Sierra Nevada-North America motion from very long baseline interferometry: Implications for the kinematics of the western United States, *Geol., 19*, 1085-1088, 1991a.

Argus, D.F., and R.G. Gordon, No-net rotation model of current plate velocities incorporating plate motion model NUVEL-1, *Geophys. Res. Lett., 18*(11), 2039-2042, 1991b.

Argus, D.F., and R.G. Gordon, Tests of the rigid-plate hypothesis and bounds on intraplate deformation using geodetic data from very long baseline interferometry, *J. Geophys. Res., 101*(B6), 13,555-13,572, 1996.

Atwater, T., Implications of plate tectonics for the Cenozoic tectonic evolution of western North America, *Geol. Soc. Am. Bull., 81*, 3513-3536, 1970.

Bakun, W.H., Seismic activity of the San Francisco Bay Region, *Bull. Seis. Soc. Am., 89*(3), 764-769, 1999.

Bennett, J.H., and R.W. Sherburne, The 1983 Coalinga, California Earthquake, pp. 335, Calif. Dep. of Conserv., Div. of Mines and Geol., Sacramento, Calif., 1983.

Bennett, R.A., B.P. Wernicke, and J.L. Davis, Continuous GPS measurements of contemporary deformation across the northern Basin and Range province, *Geophys. Res. Lett., 25*(4), 563-566, 1998.

Boucher, C., Z. Altamini, M. Feissel, and P. Sillard, Results and analysis of the ITRF94, *IERS Tech. Note 20*, Observatoire de Paris, 1996.

Chinnery, M., Deformation of the ground around surface faults, *Bull. Seis. Soc. Am., 51*, 1961.

DeMets, C., and T.H. Dixon, New kinematic models for Pacific--North America motion from 3 Ma to present, 1, Evidence for steady motion and biases in the NUVEL-1A model, *Geophys. Res. Lett., 26*(13), 1921-1924, 1999.

DeMets, C., R.G. Gordon, D.F. Argus, and S. Stein, Effect of recent revisions to the geomagnetic reversal timescale on estimates of current plate motions, *Geophys. Res. Lett., 21*(20), 2191-2194, 1994.

Dixon, T.H., S. Robaudo, J. Lee, and M.C. Meheis, Constraints on present-day Basin and Range deformation from space geodesy, *Tectonics, 14*(4), 755-772, 1995.

Dong, D., T.A. Herring, and R.W. King, Estimating regional deformation from a combination of space and terrestrial geodetic data, *J. Geod., 72*, 200-214, 1998.

Freymueller, J.T., M.H. Murray, and D. Castillo, Kinematics of the Pacific-North America plate boundary zone, northern California, *J. Geophys. Res., 104*(4), 7419-7441, 1999.

Jennings, C.W., Fault activity map of California with locations and ages of recent volcanic eruptions, Calif. Dep. of Conserv., Div. of Mines and Geol., Sacramento, Calif., 1994.

Johnson, H.O., and D.C. Agnew, Monument motion and measurements of crustal velocities, *Geophys. Res. Lett., 22*, 2905-2908, 1995.

Lisowski, M., J.C. Savage, and W.H. Prescott, The velocity field along the San Andreas fault in central and southern California, *J. Geophys. Res., 96*(B5), 8369-8388, 1991.

Prescott, W.H., and S.-B. Yu, Geodetic measurement of horizontal deformation in the northern San Francisco Bay region, California, *J. Geophys. Res.*, *91*(B7), 7475-7484, 1986.

Snay, R.A., and N.D. Weston, Future directions of the national CORS system, in paper presented at the 55th Annual Meeting of the Institute of Navigation, Inst. of Navigation, Cambridge, Mass., 1999.

Thatcher, W., G.R. Foulger, B.R. Julian, J. Svarc, E. Quilty, and G.W. Bawden, Present-day deformation across the Basin and Range Province, western United States, *Science*, *283*, 1714-1718, 1999.

Williams, S.D.P., Current motion on faults of the San Andreas system in central California inferred from recent GPS and terrestrial survey measurements, Ph.D. thesis, Univ. of Durham, Durham, England, 1995.

Wolfram, S., *Mathematica*, Cambridge Univ. Press, New York, 1996.

Working Group on California Earthquake Probabilities, Earthquake probabilities in the San Francisco Bay Region: 2000 to 2030 A summary of findings, 51 pp., *Open File Rep. 99-517*, U.S. Geol. Surv., Reston, VA, 1999.

Zumberge, J.F., M.B. Heflin, D.C. Jefferson, M.M. Watkins, and F.H. Webb, Precise point positioning for the efficient and robust analysis of GPS data from large networks, *J. Geophys. Res.*, *102*(B3), 5005-5018, 1997.

D. Manaker, Department of Geology, 174 Physics/Geology Building, University of California, One Shields Avenue, Davis, CA 95616-8605.

W.H. Prescott, J.C. Savage, and J. L. Svarc, U.S. Geological Survey, 345 Middlefield Road, MS/977, Menlo Park, CA 94025-3591. (wprescott@usgs.gov)

(Received January 25, 2000; revised October 26, 2000;
accepted October 30, 2000.)